BARRIER ENGINEERED QUANTUM DOT INFRARED PHOTODETECTORS

Sanjay Krishna

Center for High Technology Materials
Department of Electrical Engineering
University of New Mexico
1313 Goddard SE
Albuquerque, NM 87106

1 Jun 2015

Final Report

AIR FORCE RESEARCH LABORATORY
Space Vehicles Directorate
3550 Aberdeen Ave SE
AIR FORCE MATERIEL COMMAND
KIRTLAND AIR FORCE BASE, NM 87117-5776

DTIC COPY
NOTICE AND SIGNATURE PAGE

Using Government drawings, specifications, or other data included in this document for any purpose other than Government procurement does not in any way obligate the U.S. Government. The fact that the Government formulated or supplied the drawings, specifications, or other data does not license the holder or any other person or corporation; or convey any rights or permission to manufacture, use, or sell any patented invention that may relate to them.

This report is the result of contracted fundamental research deemed exempt from public affairs security and policy review in accordance with SAF/AQR memorandum dated 10 Dec 08 and AFRL/CA policy clarification memorandum dated 16 Jan 09. This report is available to the general public, including foreign nationals. Copies may be obtained from the Defense Technical Information Center (DTIC) (http://www.dtic.mil).

AFRL-RV-PS-TR-2015-0111 HAS BEEN REVIEWED AND IS APPROVED FOR PUBLICATION IN ACCORDANCE WITH ASSIGNED DISTRIBUTION STATEMENT.

//SIGNED//   //SIGNED//
DAVID CARDIMONA   PAUL D. LEVAN, Ph.D.
Program Manager   Technical Advisor, Space Based Advanced Sensing
                                                  and Protection

//SIGNED//
JOHN BEAUCHEMIN
Chief Engineer, Spacecraft Technology Division
Space Vehicles Directorate

This report is published in the interest of scientific and technical information exchange, and its publication does not constitute the Government's approval or disapproval of its ideas or findings.

REPORT DOCUMENTATION PAGE

1. REPORT DATE *(DD-MM-YY)* 01-06-2015	2. REPORT TYPE Final Report	3. DATES COVERED *(From - To)* 22 Nov 2011 – 22 May 2012
4. TITLE AND SUBTITLE Barrier Engineered Quantum Dot Infrared Photodetectors		**5a. CONTRACT NUMBER** FA9453-12-1-0336
		5b. GRANT NUMBER
		5c. PROGRAM ELEMENT NUMBER 63401F
6. AUTHOR(S) Sanjay Krishna		**5d. PROJECT NUMBER** 2181
		5e. TASK NUMBER PPM00017401
		5f. WORK UNIT NUMBER EF125327
7. PERFORMING ORGANIZATION NAME(S) AND ADDRESS(ES) Center for High Technology Materials Department of Electrical Engineering University of New Mexico 1313 Goddard SE Albuquerque, NM 87106		**8. PERFORMING ORGANIZATION REPORT NUMBER**
9. SPONSORING / MONITORING AGENCY NAME(S) AND ADDRESS(ES) Air Force Research Laboratory Space Vehicles Directorate 3550 Aberdeen Ave., SE Kirtland AFB, NM 87117-5776		**10. SPONSOR/MONITOR'S ACRONYM(S)** AFRL/RVSS
		11. SPONSOR/MONITOR'S REPORT NUMBER(S) AFRL-RV-PS-TR-2015-0111

12. DISTRIBUTION / AVAILABILITY STATEMENT
Approved for Public Release; Distribution is Unlimited.

13. SUPPLEMENTARY NOTES

14. ABSTRACT
To investigate barrier engineered designs to reduce the dark current in quantum dot infrared photodetectors using various types of barriers including confinement enhancement (CE) design.

15. SUBJECT TERMS
unipolar, barrier, infrared, detector

16. SECURITY CLASSIFICATION OF:			17. LIMITATION OF ABSTRACT	18. NUMBER OF PAGES	19a. NAME OF RESPONSIBLE PERSON David Cardimona
a. REPORT Unclassified	**b. ABSTRACT** Unclassified	**c. THIS PAGE** Unclassified	Unlimited	16	**19b. TELEPHONE NUMBER** *(include area code)*

(This page intentionally left blank)

TABLE OF CONTENTS

Section **Page**

(This page intentionally left blank)

1.0 SUMMARY
In this proposal, we wish to investigate barrier engineered designs to reduce the dark current in quantum dot infrared photodetectors. There is an increased emphasis in realizing High Operating Temperature (HOT) infrared photodetectors and the key is a reduction in the dark current. This one year effort will include a systematic study using various types of barriers including confinement enhancement (CE) design.

2.0 INTRODUCTION
In this project, we have investigated optical properties and device performance of sub-monolayer quantum dots infrared photodetector with confinement enhancing (CE) barrier and compared with conventional Stranski-Krastanov quantum dots with a similar design. This quantum dots-in-a-well structure with CE barrier enables higher quantum confinement and increased absorption efficiency due to stronger overlap of wavefunctions between the ground state and the excited state. Normal incidence photoresponse peak is obtained at $7.5\,\mu m$ with a detectivity of $1.2 \times 10^{11}\,cm\,Hz^{1/2}\,W^{-1}$ and responsivity of $0.5\,A/W$ ($77\,K$, $0.4\,V$, f/2 optics). Using photoluminescence and spectral response measurements, the bandstructure of the samples were deduced semi-empirically.

In the recent past, quantum dots (QD) infrared photodetectors based on Stranski-Krastanov (SK) QD have been extensively researched due to the advantages of the three dimensional confinement of carriers which provide intrinsic sensitivity to normal incidence radiation lower dark current and long excited state lifetime. Several groups have contributed to the drastic improvement of infrared photodetectors by introducing different material compositions and novel architectures like quantum dots in-a-well (DWELL) quantum dots in double well (DDWELL) and successfully demonstrated high performance devices. A typical DWELL structure, where InAs quantum dots are confined inside a InGaAs-GaAs quantum well (QW) offers the advantage of tuning the detection peak wavelength, while providing lower dark current and higher operating temperature. In order to increase the absorption quantum efficiency (QE) and confinement of electron wave-function, confinement enhancing (CE) barriers surrounding the dots have been introduced recently. Barve et al. (Appendix, #6) suggest a different architecture, where a $2\,nm$ thick Al0.22Ga0.78 CE barriers are employed around the entire DWELL structure. Presence of such blocking layers in the transport direction reduces the dark current significantly while providing the advantages of enhanced absorption coefficient and high escape probability.

While a considerable effort has been made to improve the barrier design, very few studies have been done beyond the idea of SK QD. Due to the nature of formation, SK dots always have an InAs wetting layer, which actually reduces the degree of confinement of carriers and does not contribute to the normal incidence absorption. Sub-monolayer (SML) QD based design has emerged as a promising solution of this problem SML QD structure is typically grown by depositing fraction of a monolayer of InAs in a GaAs or InGaAs QW. In this way, the formation of any wetting layer is avoided which causes better quantum confinement and increased carrier wave-function overlap.

Moreover, such SML QD offers higher density of dots due to smaller (∼5 nm) lateral size and narrow average lateral spacing (∼2 nm) between two dots which leads to a higher absorption efficiency. Several reports of SML QD based lasers can be found in the literature, but there are only a few reports on a SML QD infrared photodetector. The typical operating bias for SML QD detector, which is less than 1 V, is suitable for focal plane array (FPA) applications. Performance of SML QD based device can be further improved by planting the dots into a CE DWELL structure to reduce the operating bias while maintaining good absorption quantum efficiency. In this paper, we report on a SML QD in a confinement enhanced DWELL structure operating at 77 K with a detection peak wavelength of 7.5 μm with a high detectivity of 1.2×10^{11} cm Hz$^{1/2}$ W^{-1} at only 0.4 V operating bias. Absorption quantum efficiency is measured to be 7.0% at the same applied bias. We have also compared the performance of the above mentioned device with a device based on SK QD with the similar heterostructure.

The sample under consideration is grown by molecular beam epitaxy (MBE) equipped with As2 cracker source on a semi-insulating GaAs (0 0 1) substrate. We have performed a systematic study on InAs SML, including optimization of different growth parameters like the flux ratio, growth temperature, thickness of InAs deposition, and variations using different material compositions. The active region of the sample, as shown in Figure 1(a), consists of four vertically stacked 0.3ML InAs layers inside a 4.3 nm thick In0.15Ga0.85As QW, surrounded by 1 nm GaAs QW—2 nm Al0.22Ga0.78As CE barrier—48 nm Al0.07Ga0.93As barrier. This stack is repeated 10 times. Initially, the 50 nm Al0.07Ga0.93As barrier and CE barrier were grown and capped with 1 nm GaAs layer at 590 °C. Then the substrate temperature was reduced to 500 °C to grow InGaAs QW with Si doped InAs SML QD with 10 s interruption time before and after each InGaAs and InAs deposition. Then, the structure was covered with 1 nm GaAs layer and the temperature was raised to 590 °C with interruption of 180 s. The CE barrier is designed such that the excited energy level in the QW is close to the continuum energy level, which provides high absorption efficiency, high escape probability, and low bias operation. We have chosen another sample with same design with conventional SK QD instead of SML dots to compare the optical property and device performance.

3.0 METHODS, ASSUMPTION, AND PROCEDURES
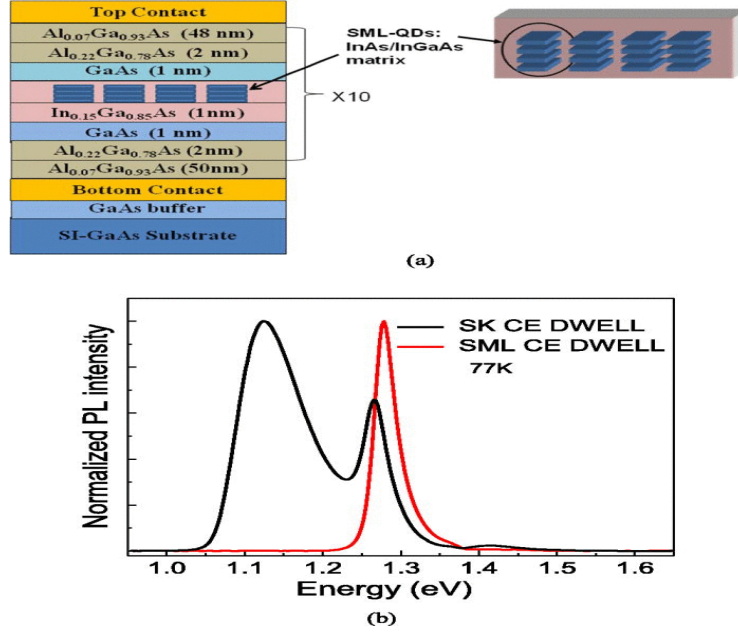
Figure 1. (a) Schematic of SML CE DWELL heterostructure. Four stacks of InAs are deposited in InGaAs matrix. (b) Comparison of normalized PL spectra of SML CE DWELL QD and SK CE DWELL QD.

In figure 1(a) InAs/InGaAs structure is embedded in GaAs quantum well and surrounded by $Al0.22Ga0.78As$ CE barrier. To obtain information about the bandstructure of our samples, we have performed room temperature photoluminescence (PL) measurements. The experiment was done using Ar++ laser with power of 2 W and InGaAs detector. Figure 1(b) depicts normalized PL spectra obtained from the SML QD and SK QD samples. The ground state of SML QD shifts towards shorter wavelength ccompared to SK QD due reduced size of dots. Note in figure 2 (b) that the ground state of SML QD coincides with 1st excited state of SK QD. For SK QD, the ground state emission peak is at 1.12 eV while the ground state emission peak for SML QD is observed at 1.28 eV. The observed blue shift in the ground state PL peak is possibly due to lesser Indium in the SML QD (~1.2ML) compared to the SK QDs (2-2.4ML). The narrower full-width-half-maximum (FWHM) of PL spectrum of SML QD suggests high uniformity of the QD size distribution. Fluence dependent PL experiment confirms the existence of the 1st excited state in SK QD which appears at 1.27 eV. It should be noted that the ground state energy level of SML QD is close to the energy level of 1st excited state of SK QD.

Devices were processed into 410×410 µm2 square detectors using a standard method of optical lithography, plasma etching, and contact metallization. A liquid nitrogen cooled cryostat and Nicholet 550 Fourier transform infrared spectrometer were used to measure the spectral response at 77 K. Figure 2(a) depicts the comparison of spectral response from SK dots and SML dots in the CE DWELL architecture. While the photocurrent response from the SK QD shows two main peaks at 6.5 µm and 7.5 µm, the SML QD sample shows response at 7.5 µm only. In figure 2 (b)

The origin spectral response peaks for SK QD is transition between ground state and excited state of the QD and the excited state in the QW. The spectral response for SML QD obtained due to the transition between ground state of the QD to the excited state in the QW. The detailed analysis of SK dots in CE DWELL is reported elsewhere. The photocurrent peak of SML QD shows a symmetric behavior for the both polarities of applied bias voltage. The peak at 7.5 µm for SK QD is identified as the transition between the excited state of the QD (E1) to the excited state in the QW. The origin of 7.5 µm in SML QD is due to the transition between the ground state of the QD (E0) to the excited state in the QW. Appearance of photocurrent response peak at 7.5 µm for both samples supports our conclusions from PL measurement. Combining the information from PL experiment and spectral response measurement, we have semi-empirically reconstructed the bandstructures of heterostructures which are shown in Figure 2(b).
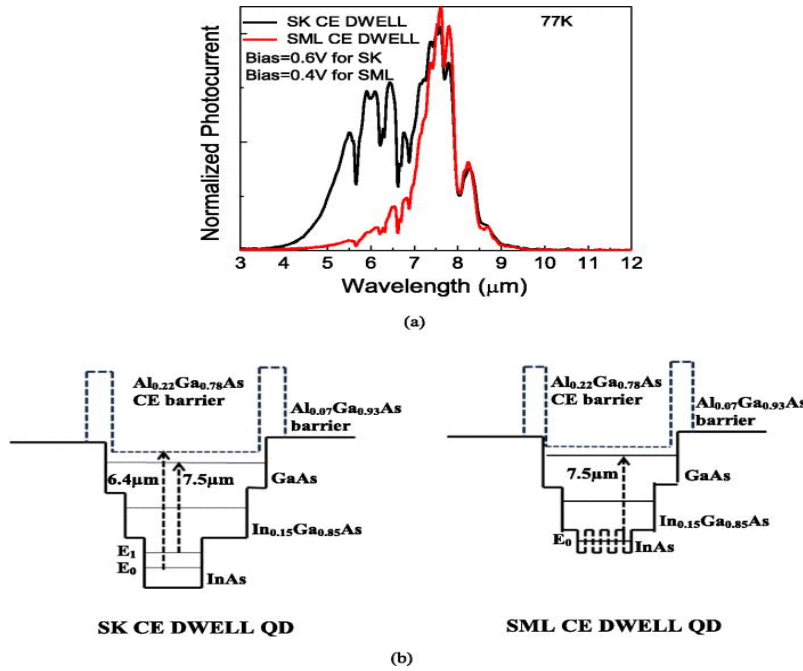

Figure 2. (a) Spectral response comparison between SML CE DWELL QD and SK CE DWELL QD at 77 K. (b) The bandstructures of SML CE DWELL QD and SK CE DWELL QD samples, constructed on the basis of PL and spectral response measurements.

Radiometric measurements were carried out by using a blackbody source calibrated at 900 K to measure detectivity (D*) and responsivity (R) of the devices at 77 K. The D* and R are calculated using the following equations:

$$D^* = R(A\Delta f)^{1/2} \text{ and } R = eg\eta/(h\nu) \tag{1}$$

where A is area of the detector, Δf is band-width, in is noise current, e is electronic charge, g is photoconductive (PC) gain, η is absorption quantum efficiency, and $h\nu$ is photoexcitation energy. By comparing the measured photocurrent with the dark current, both the devices were found to be background limited infrared photodetector (BLIP) at 77 K. In Figure 3(a), results of D* measurement are shown. The highest D* for SML QD is found to be 1.2×10^{11} cm Hz$^{1/2}$ W^{-1} at

0.4 V bias voltage, which is higher than previously reported results for SML QD although at a lower operating bias. The recorded D* for SML QD is found as a factor of two higher than the SK QD device. Figure 3(b) compares the responsivity of two devices, which shows a significant improvement of R over the whole bias range. As the detection peak is due to the transition between bound state in QD and excited energy in the QW, which is close to the continuum energy level, the escape probability of photocarriers is higher. This results in low value of operational bias and high responsivity. Responsivity of SML QD is found to be more than 4 times higher than that if SK QD at a same bias. High responsivity also indicates high value of absorption QE. The noteworthy low operating bias voltage indicates its feasibility for fabrication of FPA using commercially available silicon read-out circuits.
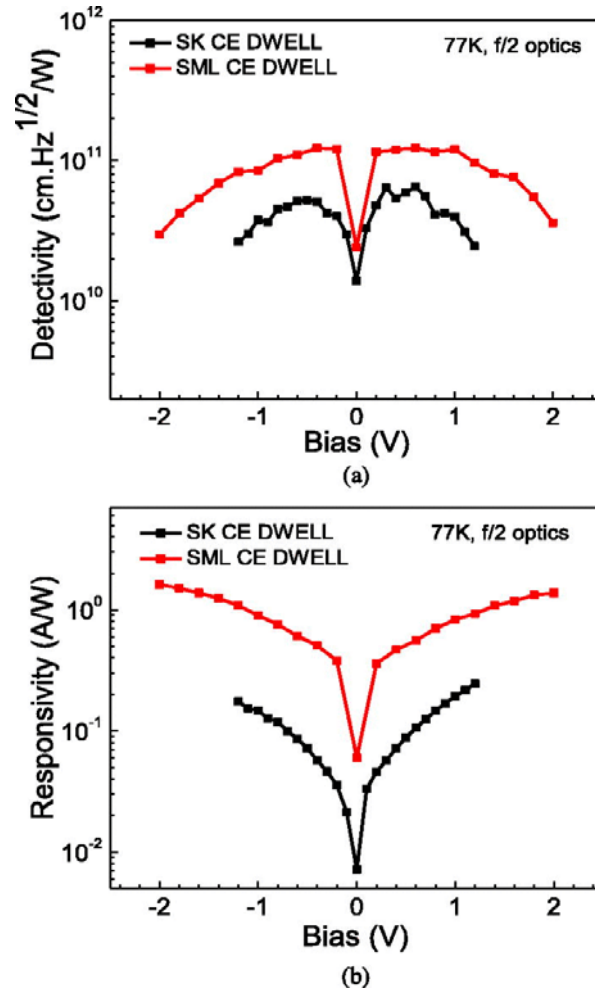
Figure 3. (a) Comparison of detectivity measurements between SML CE DWELL QD and SK CE DWELL QD (77 K, f/2 optics), showing an improvement in D* value for SML CE DWELL QD device. (b) Responsivity measurements of SML CE DWELL QD and SK CE DWELL QD samples (77 K, f/2 optics).

4.0 RESULTS AND DISCUSSIONS

To understand the transport mechanism inside the SML QD device we measured the photoconductive gain to estimate absorption QE of SML QD device. The device was irradiated by a blackbody source at 900 K during the measurement of the PC gain to ensure the device was photon noise limited. The PC gain is calculated using the following equation:

$$Gph = i2n/(4e\Delta fIph) \tag{2}$$

where in, e, Δf, and Iph are noise current, electronic charge, noise band-width, and photocurrent, respectively. Figure 4(a) shows the results of PC gain and absorption quantum efficiency at 77 K. The PC gain is found to be lower than unity at operating bias region. Due to probable existence of excited states in QW, the capture probability is high which justifies such low value of PC gain. The absorption efficiency reaches to around 7.0% at the operating bias and increases up to 11.5% as bias is increased further. Such high value of absorption QE is attributed to strong overlap of electronic wavefunction inside the dots. In addition to the presence of AlGaAs layer, the smaller size of the dots is responsible for the better wavefunction coupling which enhances the absorption strength of ground state electrons. Figure 4(b) clearly indicates a considerable enhancement in absorption QE for SML CE DWELL compared to its SK counterpart. High values of detectivity, PC gain, and absorption QE are obtained even at zero bias. This is due to the limitation of measurement setup during noise measurement and hence those results are ignored. A notable enhancement is found in absorption efficiency for SML CE DWELL.
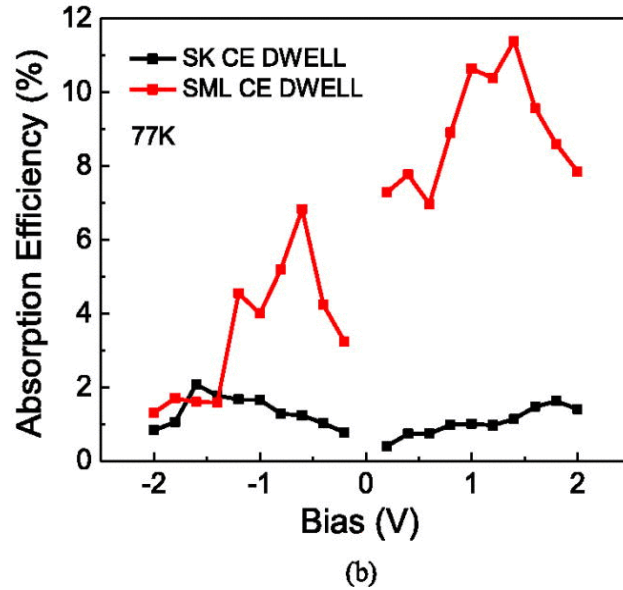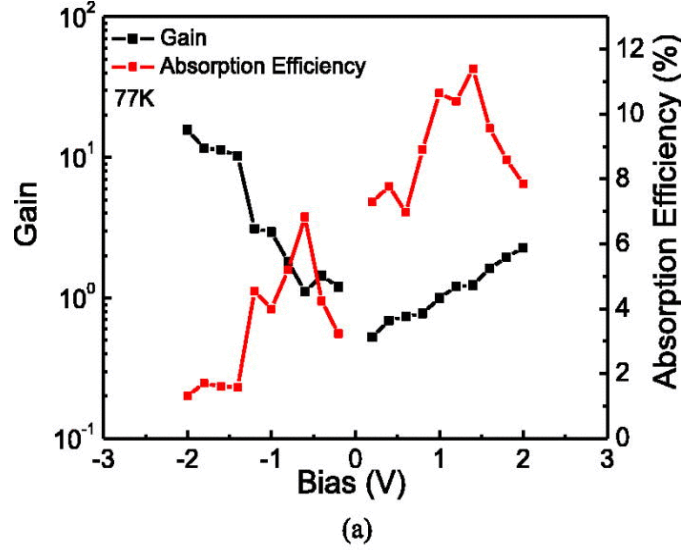
Figure 4. (a) Results of photoconductive gain and absorption efficiency measurement of SML CE DWELL is shown. (b) Comparison of absorption efficiency measurement of SML CE DWELL QD and SK CE DWELL QD.

5.0 CONCLUSIONS

In conclusion, infrared photodetector based on SML QD has been presented and compared with traditional SK QD in CE DWELL architecture. Our design of SML QD exhibits better performance compared to previously recorded citations. We have also investigated the optical properties of SML QD to understand the structure of different energy levels. The device characterization results ensure high performance at low operating bias at 77 K. Higher confinement and better overlap of wavefunctions between the ground state of the quantum dot and excited state of the quantum well are achieved owing to the presence of CE barrier and smaller size of dots. Detectivity of the SML based device is measured as 1.2×10^{11} cm Hz1/2 W−1 with responsivity reaching up to 0.5 A/W (77 K, 0.4 V, 7.5 μm, f/2 optics).

Appendix: Publications resulting from this effort

In this project, there were barrier engineered detectors that were explored. The scope of the project was expanded to include Type II superlattice detectors. A list of the publications resulting from this work is shown below.

1. Schuler-Sandy, T., S. Myers, B. Klein, N. Gautam, P. Ahirwar, Z-B. Tian, T. Rotter, G. Balakrishnan, E. Plis, and S. Krishna. "Gallium free type II InAs/InAsSb superlattice photodetectors." Applied Physics Letters 101, no. 7 (2012).
2. Plis, E., N. Gautam, B. Klein, S. Myers, T. Schuler-Sandy, M. N. Kutty, Z-B. Tian, and S. Krishna. "Performance of single-and dual-color detectors using InAs/GaSb strained layer superlattices." In Lester Eastman Conference on High Performance Devices (LEC), 2012, pp. 1-4. IEEE, 2012.
3. Plis, Elena, Brianna Klein, Stephen Myers, Nutan Gautam, and Sanjay Krishna. "(111) InAs/GaSb type-II strained layer superlattice material for high operating temperature detection." physica status solidi (c) (2013).
4. Sengupta, S., J. O. Kim, A. V. Barve, S. Adhikary, Y. D. Sharma, N. Gautam, S. J. Lee, S. K. Noh, S. Chakrabarti, and S. Krishna. "Sub-monolayer quantum dots in confinement enhanced dots-in-a-well heterostructure." Applied Physics Letters 100, no. 19 (2012).
5. Cowan, V. M., C. P. Morath, J. E. Hubbs, S. Myers, E. Plis, and S. Krishna. "Radiation tolerance characterization of dual band InAs/GaSb type-II strain-layer superlattice pBp detectors using 63 MeV protons." Applied Physics Letters 101, no. 25 (2012): 251108-251108.
6. Barve, Ajit V., Saumya Sengupta, Jun Oh Kim, John Montoya, Brianna Klein, Mohammad Ali Shirazi, Marziyeh Zamiri et al., "Barrier selection rules for quantum dots-in-a-well infrared photodetector." Quantum Electronics, IEEE Journal of 48, no. 10 (2012): 1243-1251.
7. Cowan, V. M., C. P. Morath, J. E. Hubbs, S. Myers, E. Plis, and S. Krishna. "Radiation tolerance characterization of dual band InAs/GaSb type-II strain-layer superlattice pBp detectors using 63 MeV protons." Applied Physics Letters 101, no. 25 (2012): 251108-251108.
8. Plis, E., M. Naydenkov, S. Myers, B. Klein, N. Gautam, S. S. Krishna, E. P. Smith, S. Johnson, and S. Krishna. "Dual-band pBp detectors based on InAs/GaSb strained layer superlattices." Infrared Physics & Technology (2012).
9. Plis, E., B. Klein, S. Myers, N. Gautam, E. P. Smith, and S. Krishna. "High Operating Temperature Midwave Infrared InAs/GaSb Superlattice Photodetectors on (111) GaSb Substrates." (2013): 1-3.
10. Gautam, Nutan, Stephen Myers, Ajit Barve, Brianna Klein, E. Smith, D. Rhiger, H. Kim, Z-B. Tian, and Sanjay Krishna. "Barrier Engineered Infrared Photodetectors Based on Type-II InAs/GaSb Strained Layer Superlattices." (2013): 1-1.

Personnel Impact

Two of the students working on this project, Nutan Gautam and Stephen Myers, have completed their PhD. Dr. Gautam is at University of California Santa Barbara and Dr. Myers is at SKINfrared, a UNM based start-up.

LIST OF ACRONYMS

BLIP	Background limited infrared photodetector
CE	Confinement enhancement
D*	Detectivity
DWELL	Dots in-a-well
DDWELL	Double dots in-a-well
FPA	Focal plane array
FWHM	Full-width-half-maximum
HOT	High Operating Temperature
MBE	Molecular beam epitaxy
PC	Photoconductive
PL	Photoluminescence
QE	Quantum efficiency
QD	Quantum dots
R	Responsivity
SK	Stranski-Krastanov
SML	Sub-Monolayer

DISTRIBUTION LIST

DTIC/OCP
8725 John J. Kingman Rd, Suite 0944
Ft Belvoir, VA 22060-6218   1 cy

AFRL/RVIL
Kirtland AFB, NM 87117-5776   2 cys

Official Record Copy
AFRL/RVSS/David Cardimona   1 cy